Studsvik

STUDSVIK/N(H)-03/069 Rev. 1

Fuel Pellet Isotopic Analyses of Vandellós 2 Rods WZtR165 and WZR0058

Final report

Hans-Urs Zwicky
Jeanett Low

Studsvik Report

Restricted distribution

STUDSVIK NUCLEAR AB

STUDSVIK/N(H)-03/069 Rev. 1

2008-04-25 Rev.

60063

Hans-Urs Zwicky
Jeanett Low

ENUSA

Fuel Pellet Isotopic Analyses of Vandellós 2 Rods WZtR165 and WZR0058

Final report

Summary

In the framework of the high burnup fuel performance programme agreed between Studsvik and ENUSA, the latter representing a number of Spanish organisations, a selection of isotopes was determined by means of different techniques in two fuel rods irradiated in the Spanish reactor Vandellós 2. Radionuclides with suitable half-lives and gamma lines were determined based on axial gamma scans of the entire fuel rods. High Pressure Liquid Chromatography combined with an Inductively Coupled Plasma Mass Spectrometer (HPLC-ICP-MS) or ICP-MS without separation was applied for the analysis of individual isotopes of about 10 different elements in a total of seven different samples. In total, about 50 nuclides have been analysed by ICP-MS in each sample. In general, these over 300 data points give a consistent picture of the isotopic content of irradiated fuel as a function of burnup. Taking into account that Studsvik applied these methods for the first time in such a comprehensive project, the outcome is considered to be satisfactory. On the other hand, some systematic deviations from expectations have been identified. Moreover, the scatter of $^{n}X/^{238}U$ weight ratios of fission products that would have the potential for determining the local pellet burnup by comparison with CASMO calculations appears to be too large. Therefore, burnup values determined by comparing the isotopic abundance of ^{235}U and ^{239}Pu to CASMO based values are considered to be the most reliable ones.

Analysis of cladding samples cut out from the plenum region of rods shipped from Vandellos to Studsvik confirmed that rearrangement of rods during reception of the rods, fitting top end plug engravings to the expected pattern, led to a mix-up of the rods. The revised report correlates the performed PIE program to the real rod identities.

Reviewed by	Date	Approved by	Date
Gunnar Lysell	2008-06-13	Camilla Hoflund	2008-06-24
Gunnar Lysell		Camilla Hoflund	

Table of Contents

List of Tables

List of Figures

1 Introduction

In the framework of the high burnup fuel performance programme agreed between Studsvik and ENUSA, the latter representing a number of Spanish organisations, a selection of isotopes was determined by means of different techniques in two fuel rods irradiated in the Spanish reactor Vandellós 2. Radionuclides with suitable half-lives and gamma lines were determined based on axial gamma scans of the entire fuel rods. High Pressure Liquid Chromatography combined with an Inductively Coupled Plasma Mass Spectrometer (HPLC-ICP-MS) or ICP-MS without separation was applied for the analysis of individual isotopes of about 10 different elements in a total of seven different samples.

Analysis of cladding samples cut out from the plenum region of six rods shipped in 2001 from Vandellos to Studsvik confirmed that information on the top markings was wrong [Ref. 1]. Consequently, the rearrangement of rods performed at Studsvik during reception of the rods, fitting top end plug engravings to the expected pattern [Ref. 2], led to a mix-up of the rods. In particular, rods with cladding of ZIRLO and more pronounced radial texture were mistaken for rods with MDA cladding. In that context, it should be noted that the rods were not individually marked, except for the mismatching top markings that distinguished between different cladding types only.

The revised report correlates the performed PIE program to the real rod identities.

Rev. 0 of this report contained some results that were corrected later on by a complementary report [Ref. 3]. Erroneous data are therefore deleted in Rev. 1 and replaced by a reference to the complementary report.

2 Materials and Methods

2.1 Fuel Rods

The two rods WZtR165 and WZR0058 were irradiated in the Vandellós 2 reactor during cycles 7 to 11, between June 1994 and September 2000. They were located in two different fuel assemblies. For their last cycle, both rods were removed from their original assembly and inserted into two different positions of the same assembly. During the first four cycles, the two assemblies were located in equivalent core positions. Consequently, irradiation histories are quite similar, except for the fourth cycle of irradiation, when both assemblies sat in peripheral positions, where the different rod locations within the assembly led to a significant difference in accumulated burnup increment during this fourth cycle: 11.3 MWd/kgU for WZtR165, 2.62 MWd/kgU for WZR0058 [Ref. 4].

2.2 Released Fission Gases

The rods were punctured in the plenum. The internal gas was expanded into a standard volume and the resulting pressure was determined. Samples of the gas were collected for analysis by mass spectrometry. The total internal free volume of the rod was determined by the backfill method, using argon at constant pressure. The fission gas release fraction was calculated from the experimentally determined amount of Xe and Kr extracted from the rod and the ORIGEN calculated total inventory of Xe and Kr generated in the fuel over its entire irradiation. A more detailed description of the method and of the data evaluation can be found in [Ref. 5].

As only the amount of fission gases released to the free volume of the fuel rod is analysed by this method, the results are not directly related to the results of other analyses performed in the framework of this project.

2.3 Axial Gamma Scans

2.3.1 Method

A high purity germanium detector behind a 0.5 mm tungsten collimator was used for the measurements. Axial gamma scanning was performed applying the technique of closely spaced point measurements. Nuclide specific activity values per length unit [Bq/mm] were determined based on the scan of a well characterised reference rod. Details of the method are described in [Ref. 6].

2.3.2 Measurements

The full length rods were cut into four segments after puncturing for fission gas release analysis, keeping track of the circumferential orientation of the individual segments relative to each other. A special holder was used. It

grips the rod segments in the top end. The holder caused a shielding effect of approximately 1 cm. The rods WZtR165 (complete rod) and WZR0058 (up to about 3400 mm from lower end of fuel column) were scanned for isotopes ^{95}Nb, ^{103}Ru (WZtR165 only), ^{106}Ru, ^{154}Eu, ^{134}Cs, ^{137}Cs, ^{144}Ce, ^{144}Pr. The distance between individual measurements was 0.5 mm for rod WZR0058 and 0.25 mm for rod WZtR165.

2.3.3 Transformation into Amount ^{n}X relative to ^{238}U

In order to compare the results of axial gamma scan and isotope dilution analysis, the gamma scan results were transformed into amount of nuclide ^{n}X in weight percent relative to ^{238}U according to the following procedure:

- From the region of the axial segments cut out for radiochemical analysis, the average activity per length unit [Bq/mm] is calculated from the data reported in [Ref. 6] over two pellets for samples E58-88, -148 and -263, over four pellets for the other samples.
- Based on the basic formula for radioactivity ($A = N\lambda$), the amount of nuclide ^{n}X per length unit [µg/mm] is calculated.
- The amount of ^{238}U per length unit [µg/mm] of unirradiated fuel is determined, based on pre-irradiation data (density, stoichiometry, enrichment).
- The change in the amount of ^{238}U per length unit during irradiation is estimated based on CASMO calculations, neglecting the irradiation-induced change of the fuel stack length, which uses to be less than 1 %.
- The amount of nuclide ^{n}X in weight percent relative to ^{238}U is calculated by dividing the amount of nuclide ^{n}X per length unit by the amount of ^{238}U per length unit.

2.4 Radiochemical Analyses

2.4.1 Selected Samples

Samples from four different burnup levels were selected from rod WZR0058, based on the axial ^{137}Cs profile. At the highest level, three samples with the same nominal burnup, all within 23 mm, were chosen. From rod WZtR165, only one sample was selected. Table 1 shows an overview and the designation of the samples.

Table 1 Analysed samples

Rod	WZR0058						WZtR165
Sample	E58-88	E58-148	E58-263	E58-773	E58-793	E58-796	WZtR165-2a
Cutting Position [mm](1)	88	148	263	773	793	796	1060
Burnup [MWd/kgU](2)	41	52	63	74	74	74	75

(1) From bottom end of rod
(2) Based on gamma scanning

2.4.2 Dissolution

A fuel rod slice of about 2 mm was placed in a glass flask together with 20 ml of concentrated HNO_3 and kept at 65°C for 6 h. Evaporation of liquid was avoided by means of an air-cooled reflux cooler. Nitrogen was bubbled through the liquid in order to stir it. The fuel matrix together with all fission products of interest went into solution. The cladding and the metallic fission product inclusions remained undissolved.

In the order of 0.1-0.4 g of the original fuel solution was diluted into 100 ml of HNO_3 (7.5 M) in the hotcell. 20 ml of this solution were transferred to the laboratory. An appropriate aliquot is diluted with 100 ml HNO_3 (0.16 M) to a target uranium concentration of about 4 ppm. The uranium concentration is determined by Scintrex analysis. The Scintrex UA-3[1] is a uranium analyser, measuring the characteristic fluorescence of the uranyl ion in solution after irradiation with a very short pulse of ultraviolet light from a nitrogen laser. 30 g of this mother solution is then mixed with all necessary spike solutions.

2.4.3 The HPLC-ICP-MS Instrument

A DIONEX DX300 High Performance Liquid Chromatography system with an IonPac CG10 (4 x 50 mm) guard and an IonPac CS10 (4 x 250 mm) analytical column was used for the separations. The eluents were directly injected into a VG ELEMENTAL Plasmaquad PQ2+ Inductively Coupled Plasma Mass Spectrometer (ICP-MS), installed in a glove box. Details can be found in [Ref. 7].

2.4.4 ICP-MS Analysis Based on One-Point Calibration

In this mode of analysis, count rates from an aliquot of the mother solution that is diluted as appropriate were compared to count rates from multi-element standard solutions. The first step in the evaluation of the data consisted of normalising all count rates to each other by means of added internal standards (^{115}In for fission products, ^{209}Bi for actinides). Blank corrections were

[1] SCINTREX UA-3 Uranium Analyser, SCINTREX, Snidercroft Road, Concord Ontario Canada L4K 1B5

performed by means of measurements of a pure diluted HNO_3 solution (0.16 M) preceding the analysis of each sample and standard solution. Average values were then compared to the corresponding average values measured in the standard solutions. By means of the known concentration of the nuclide in the standard the concentration of the nuclide in the sample was calculated.

This mode of analysis is restricted to isotopes without any isobaric overlap. ^{133}Cs, ^{135}Cs, ^{237}Np as well as ^{244}Cm and ^{246}Cm were determined by analysis based on one-point calibration. The error estimation was amongst others based on a comparison with the IDA results for interference-free nuclides determined by both methods.

2.4.5 Isotope Dilution Analysis

Basis

Isotope Dilution Analysis (IDA) is based on the addition of a known amount of an enriched isotope ("spike") to a sample. Isotopic ratios between the added isotope and the isotope to be analysed are determined by mass spectrometry in the mixture of spike and sample, in the sample and, if not already known, in the spike. The amount of the isotope to be determined in the sample can be calculated according to the method derived below:

$a = spike\ isotope$

$b = isotope\ to\ be\ analysed$

$R_s = isotope\ ratio\ (a/b)\ in\ sample$

$R_{Sp} = isotope\ ratio\ in\ spike$

$R_M = isotope\ ratio\ in\ mixture$

$N_a^S = number\ of\ \ isotope\ a\ in\ sample$

$N_a^{Sp} = number\ of\ \ isotope\ a\ in\ spike$

$N_b^S = number\ of\ \ isotope\ b\ in\ sample$

$N_b^{Sp} = number\ of\ \ isotope\ b\ in\ spike$

$$R_s = \frac{N_a^S}{N_b^S} \tag{1}$$

$$R_{sp} = \frac{N_a^{Sp}}{N_b^{Sp}} \tag{2}$$

$$R_M = \frac{N_a^S + N_a^{Sp}}{N_b^S + N_b^{Sp}} \tag{3}$$

By transforming Equation (3), the following Equation (4) can be derived:

$$N_b^S = \frac{N_a^{Sp} - R_M \times N_b^{Sp}}{R_M - R_s} \tag{4}$$

N_b^{Sp} can be substituted by means of Equation (2), which leads to Equation (5):

$$N_b^S = N_a^{Sp} \times \frac{1 - \frac{R_M}{R_{Sp}}}{R_M - R_s} \tag{5}$$

Once the amount of isotope *b* in the sample has been determined, all other isotopes of the same element can easily be determined by means of the isotopic ratios measured by mass spectrometry.

Spiking

R_S, the isotope ratio in the sample, is given. R_{Sp}, the ratio in the spike is fixed as well, once the appropriate standard is chosen for a series of analyses. R_M, the isotope ratio in the mixture, on the other hand can be influenced by the amount of spike solution that is blended with the sample aliquot. Two aspects have to be taken into account when choosing the appropriate R_M value: counting statistics, influencing the uncertainty of the isotopic ratio, and the factor that determines the contribution of the uncertainty in R_M by error propagation to the overall error of the analysis.

The approximate amount of the isotopes to be analysed in the sample as well as the corresponding R_S values were estimated based on the result of semi-quantitative analyses and on CASMO calculations. After choosing an appropriate R_M value, the number of spike isotopes to be added to an aliquot of the mother solution was calculated based on Equation (5).

Identities of spike isotopes and of isotopes to be analysed, as well as their abundance in the corresponding spike solutions, are shown in Table 2.

Table 2 Abundances of spike isotope and isotope to be analysed in spike solutions

Spike Isotope	Abundance [%]	Isotope to be analysed	Abundance [%]
^{233}U	98.043	^{238}U	0.804
^{242}Pu	99.903	^{239}Pu	0.0826
^{243}Am	99.966(1) 99.967(2)	^{241}Am	0.031(1) 0.030(2)
^{140}Ce	99.30	^{142}Ce	0.70
^{148}Nd	91.60	^{146}Nd	2.50
^{154}Sm	99.02	^{152}Sm	0.473
^{151}Eu	99.24	^{153}Eu	0.76
^{155}Gd	91.6	^{156}Gd	6.34

(1) Reference date: April 12, 1984
(2) Calculated for September 2003

IDA without Separation

Uranium isotopes were determined by IDA based on ICP-MS without separation. Aliquots of spiked and unspiked solutions were diluted as appropriate in order to avoid too large dead time corrections. The measurements were performed in the peak jump mode.

HPLC-ICP-MS

Plutonium and americium isotopes were determined by IDA based on HPLC-ICP-MS, with an elution program separating the two elements from each other and from interfering elements, e.g. uranium. Aliquots of spiked and unspiked solutions were diluted as appropriate.

In a separate run, the lanthanides cerium, neodymium, samarium, europium and gadolinium were determined, applying the corresponding elution method.

Data Evaluation

Count rates measured in the analysis of uranium, performed without any separation, were dead time and blank corrected. The count rates from the unspiked and spiked samples of mass 238 were corrected for the contribution of ^{238}Pu, based on the count rate for mass 239 and the ratio of ^{238}Pu and ^{239}Pu determined in the plutonium analysis. The abundance of uranium isotopes in the unspiked sample was determined by normalising the corresponding count rates of five individual measurements to 100%, followed by calculating an average value for each individual isotope. R_S was determined

based on the corresponding abundances; R_M was calculated directly from the corresponding count rates. The number of ^{238}U atoms was calculated according to Equation (5). For all other isotopes, the number of atoms in the sample was calculated by means of the corresponding abundances, based on the number of atoms of the isotope to be analysed.

HPLC-ICP-MS analyses were evaluated in the same way. Instead of count rates, peak areas determined by a dedicated program (MassLynx) were used as input data. In the case of HPLC-ICP-MS, only three individual measurements were performed.

The number of atoms in the sample was transformed into micrograms. Finally, the amount of nuclide ^{n}X in weight percent relative to ^{238}U was calculated by dividing the corresponding amount by the amount of ^{238}U.

Error Estimation

The uncertainty of the number of counts in a pulse counting system like ICP-MS is given by the square root of the number of counts, neglecting the contribution of the background signal. When applying the rules of error propagation on the simple equation (6) for the ratio of two isotopes of interest, it can be demonstrated that the precision of the ratio is limited by the size of the smaller peak (equation (7)).

$$r = \frac{a}{b} \tag{6}$$

with

$r = isotopic\ ratio$

$a, b = number\ of\ \ counts$

$$\frac{s_r}{r} = \sqrt{\frac{1}{a} + \frac{1}{b}} \tag{7}$$

with

$s_r = error\ of\ \ r$

Experience from routine analysis has shown that it is normally not possible to achieve a lower relative standard deviation of r than about 0.1 %, even if sufficient counts are available [Ref. 8]. If the number of counts in the smaller of the two peaks is significantly larger than 10^6, the contribution of counting statistics is negligible. This is normally the case in HPLC-ICP-MS analyses. In ICP-MS analyses in peak jump mode, numbers of counts may be smaller. With 10^5 counts in the smaller peak, the contribution of counting statistics to the relative error of r is still below 0.5 %. On the other hand,

additional factors like instrument instability limit the achievable accuracy. A possibility of assessing this scatter is calculating the relative standard deviation of the five and three abundance values of individual isotopes, respectively, in the unspiked samples that were determined by normalising the count rates of individual measurements to 100 %. For each isotopic ratio, s_r calculated by error propagation from the standard deviation of abundance values was compared to a value based on equation (7). The larger of the two values was then used in the overall error estimation.

The equation for calculating the error of the number of atoms of the isotope to be analysed in the sample (Equation (8)) is derived from Equation (5) according to the general rules of error propagation.

$$s_{N_b^S} = N_b^S \times \sqrt{\left(\frac{s_{N_a^{Sp}}}{N_a^{Sp}}\right)^2 + \left(\frac{R_S - R_{Sp}}{R_{Sp} - R_M}\right)^2 \times \left(\frac{s_{R_M}}{R_M - R_S}\right)^2 + \left(\frac{s_{R_S}}{R_M - R_S}\right)^2 + \left(\frac{R_M}{R_{Sp} - R_M}\right)^2 \times \left(\frac{s_{R_{Sp}}}{R_{Sp}}\right)^2} \quad (8)$$

with

$s_i = absolute\ error\ of\ i$

For all other isotopes, Equation (9) is applied:

$$s_{N_x} = N_x \times \sqrt{\left(\frac{s_{N_b^s}}{N_b^s}\right)^2 + \left(\frac{s_r}{r}\right)^2} \quad (9)$$

The relative error of the number of added spike atoms $\left(\frac{s_{N_a^{Sp}}}{N_a^{Sp}}\right)$ and the relative error of R_{Sp} $\left(\frac{s_{R_{Sp}}}{R_{Sp}}\right)$ used in the calculations are estimated as shown in Table 3.

Table 3 Errors of input data used in calculations

Parameter	Relative Error (Comment)
N_a^{Sp}	1 % (Estimated, same value for all elements)
R_{Sp}	
U	0.1 % (Estimated)
Pu	0.1 % (Estimated)
Am	1 % (Estimated)
Ce	1 % (Estimated)
Nd	0.5 % (Estimated)
Sm	0.5 % (Estimated)
Eu	0.5 % (Estimated)
Gd	1 % (Estimated)
R_S ,R_M, r	Determined according to the method described in the text

2.5 Burnup Determination

One of the traditional methods for determining the burnup of irradiated LWR fuel is the ^{148}Nd method according to ASTM E 321 [Ref. 9]. Probably one of the largest sources for systematic errors in this method is the assumed fission yield, requiring knowledge of the fraction of fissions occurring in ^{238}U (fast neutron fission) and ^{235}U, ^{239}Pu and ^{241}Pu (thermal). Another traditional method for burnup determination is based on the uranium and plutonium isotopic composition (ASTM E 244 [Ref. 10]); however, this method is rarely used for LWR fuel due to its rather simplified and rough assumptions regarding the neutron spectrum and fission fractions (the standard has been withdrawn in 2001). However, modern physics codes like CASMO and HELIOS are instead able to calculate the amount of fission products and actinides formed or consumed during reactor operation in a much more sophisticated way, taking changes of irradiating conditions into account in a more detailed way than in the ASTM E 321 and ASTM E 244 methods. The uncertainty of these methods can therefore be eliminated to a certain extent, if the experimentally determined amount of suitable fission products or actinides is compared to the result of, e.g., CASMO calculations. Cross sections applied for CASMO calculations of isotope number densities are in general well known, at least in the case of fission products that are candidates for being used for burnup determination. The accuracy of CASMO results depends primarily on the quality of modelling operating history. In the case of the two analysed rods, operation was well documented, thus allowing a quite detailed modelling. Therefore, the error of CASMO calculations is assumed to be smaller than experimental errors.

Based on [Ref. 4], number densities of all actinide and fission product isotopes of interest were calculated as a function of burnup by CASMO. The number densities were transformed into $^{n}X/^{238}$U values. Experimentally determined values for ^{140}Ce, ^{142}Ce, ^{145}Nd, ^{146}Nd and ^{148}Nd were compared to

the calculated values, thus allowing a determination of the local pellet burn-up. In addition, local pellet burnup was determined by comparing ^{235}U and ^{239}Pu isotopic abundances analysed by ICP-MS to isotopic abundances calculated from CASMO number densities.

3 Results and Discussion

3.1 Released Fission Gases

The results of fission gas analyses are compiled in Table 4. Background information on the data evaluation can be found in [Ref. 5].

Table 4 Results of fission gas analysis [Ref. 5]

Rod		WZtR165	WZR0058
Assumed burnup [MWd/kgU]		70.0	68.5
Assumed energy per fission [MeV]		200	200
Fission gas release [%]	Kr	7.56	7.77
	Xe	6.82	7.41
	Kr + Xe	6.88	7.43
Assumed energy per fission [MeV]		205.5	205.3
Fission gas release [%]	Kr	7.77	7.98
	Xe	7.00	7.61
	Kr + Xe	7.07	7.63
Isotopic composition of Kr [%]	^{80}Kr	0.002	0.004
	^{82}Kr	0.275	0.261
	^{83}Kr	8.392	8.554
	^{84}Kr	34.497	34.286
	^{85}Kr	5.540	5.396
	^{86}Kr	51.294	51.449
Isotopic composition of Xe [%]	^{128}Xe	0.073	0.069
	^{129}Xe	0.002	0.003
	^{130}Xe	0.239	0.223
	^{131}Xe	5.059	5.146
	^{132}Xe	24.032	23.991
	^{134}Xe	28.341	28.483
	^{136}Xe	42.253	42.085

3.2 Axial Gamma Scans

In rod WZR0058, ^{103}Ru (half-life 39.35 d) could not be measured after a cooling time of 19 months. All activities except for ^{95}Nb were corrected for the decay since the end of the irradiation. With ^{95}Zr (half-life: 64 days), ^{95}Nb (34.97 days) has a mother nuclide with a comparable half-life. Moreover, at the end of the irradiation, both nuclides were present. Consequently, it is not possible to calculate back to this point in time, based on the ^{95}Nb activity only at the time of the measurement.

Axial activity distributions of ^{103}Ru (rod WZtR165 only), ^{106}Ru, ^{134}Cs, ^{137}Cs, ^{144}Ce and ^{154}Eu are plotted in Figure 1 to Figure 6 for rod WZR0058, and in Figure 7 to Figure 13 for rod WZtR165.

^{144}Pr (half-life: 17.3 m) is the short-lived daughter of ^{144}Ce. The two nuclides are in secular equilibrium, meaning that their activities are equal. The ratio of their amounts is the same as the ratio of their half-lives. This means that the amount of ^{144}Pr is only about 4×10^{-5} times the amount of ^{144}Ce.

With an intensity of 94.4%, ^{137}Cs decays into ^{137m}Ba (half-life 2.552 m). Consequently, the ^{137m}Ba activity is 94.4% of the ^{137}Cs activity. As the half-life ratio between daughter and mother nuclide is even lower than in the case of ^{144}Ce/Pr, there are only traces of ^{137m}Ba present (1.5×10^{-7} times the amount of ^{137}Cs).

^{106}Ru (half-life 373.6 d) decays over ^{106}Rh (half-life 30 s) into ^{106}Pd (stable). Consequently, the ^{106}Rh activity is the same as the ^{106}Ru activity. The half-life ratio between daughter and mother nuclide in this case is 9.3×10^{-7}. Consequently, as in the case of ^{137m}Ba, there are only traces of ^{106}Rh in the sample.

Estimated nuclide and rod specific single point standard deviations are compiled in Table 5, estimated nuclide and rod specific overall errors in Table 6. A detailed error discussion can be found in [Ref. 6].

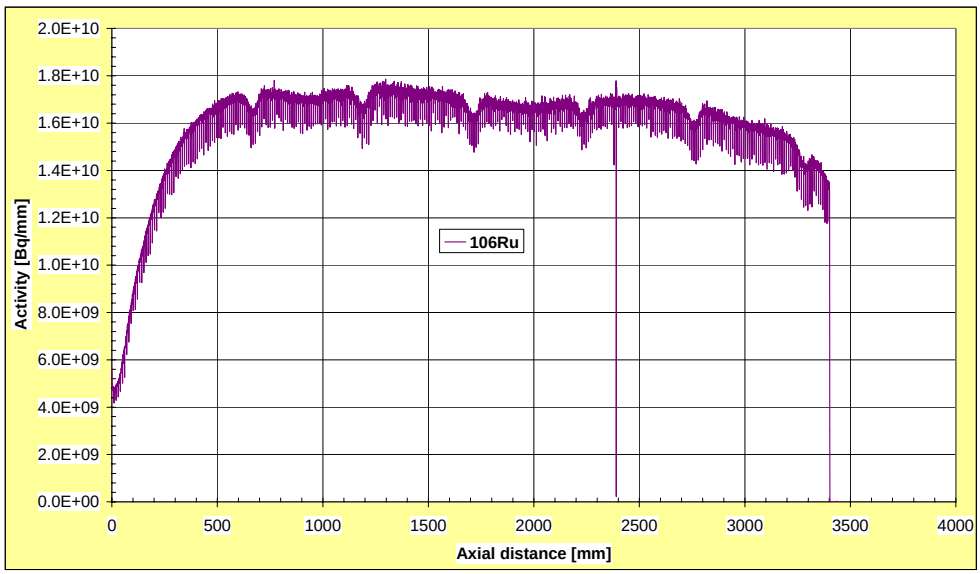

Figure 1 Rod WZR0058, axial ^{106}Ru activity distribution at the end of irradiation

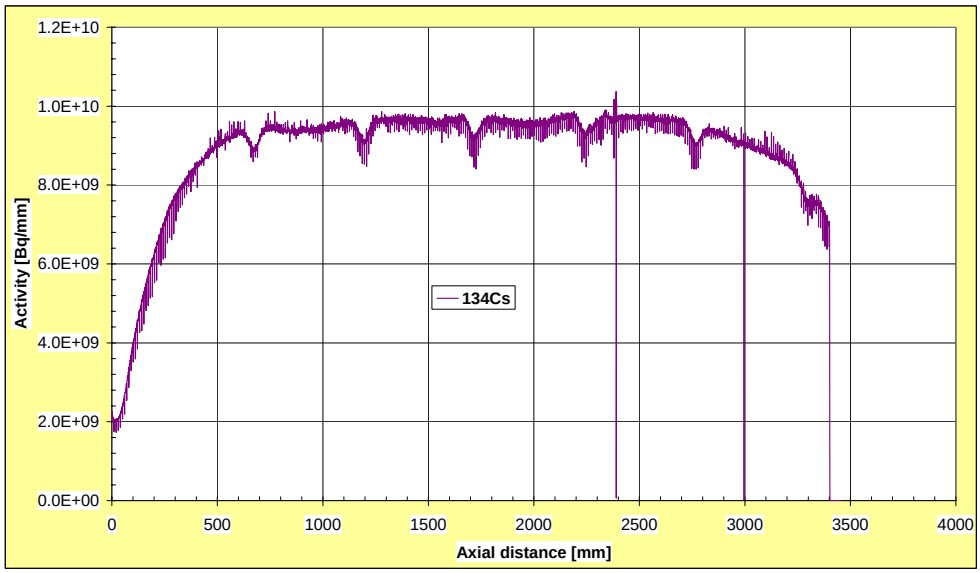

Figure 2 Rod WZR0058, axial ^{134}Cs activity distribution at the end of irradiation

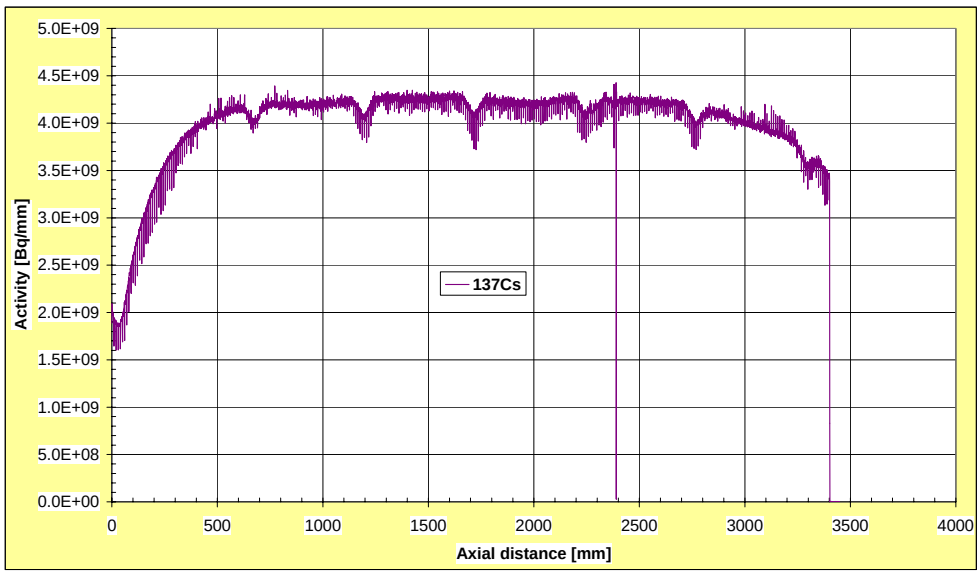

Figure 3 Rod WZR0058, axial ^{137}Cs activity distribution at the end of irradiation

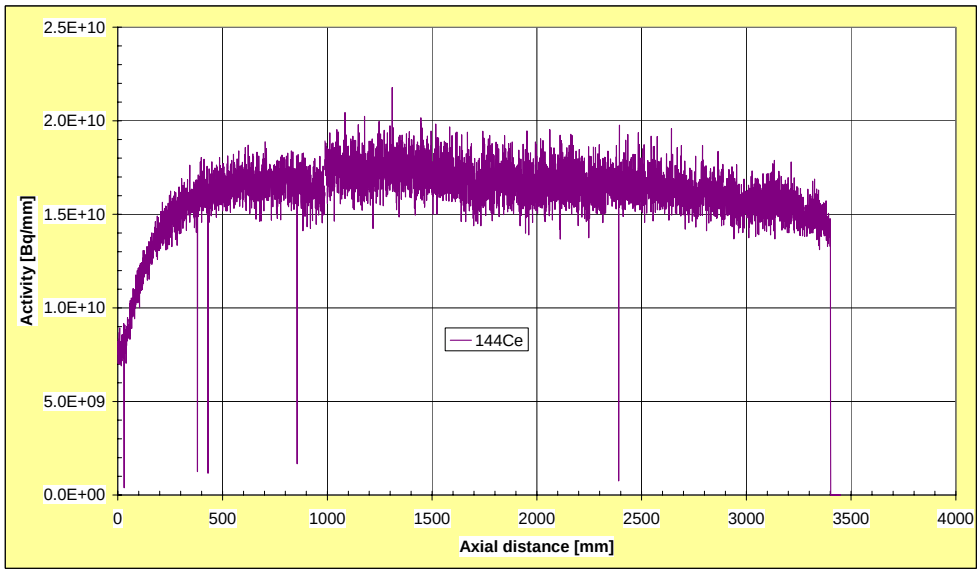

Figure 4 Rod WZR0058, axial ^{144}Ce activity distribution at the end of irradiation

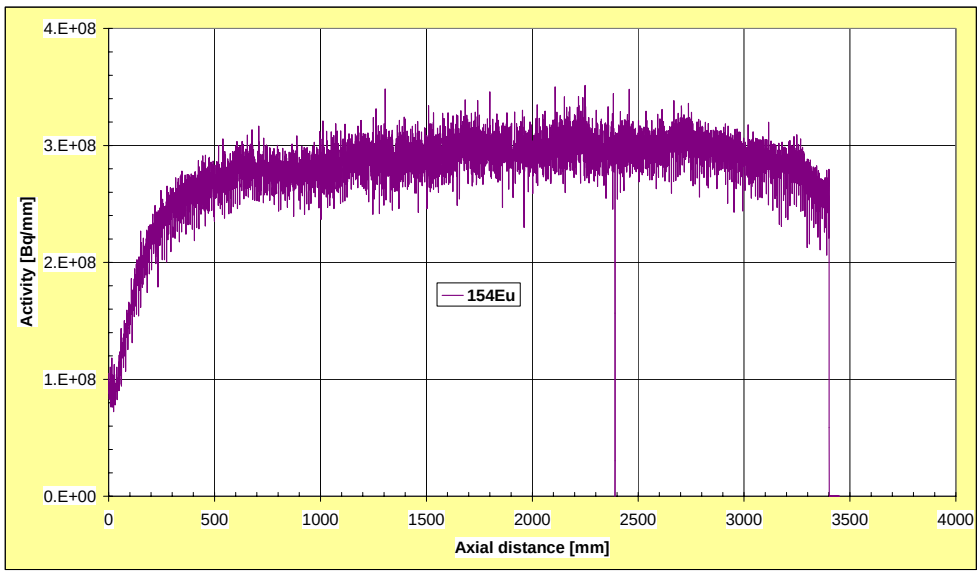

Figure 5 Rod WZR0058, axial ^{154}Eu activity distribution at the end of irradiation

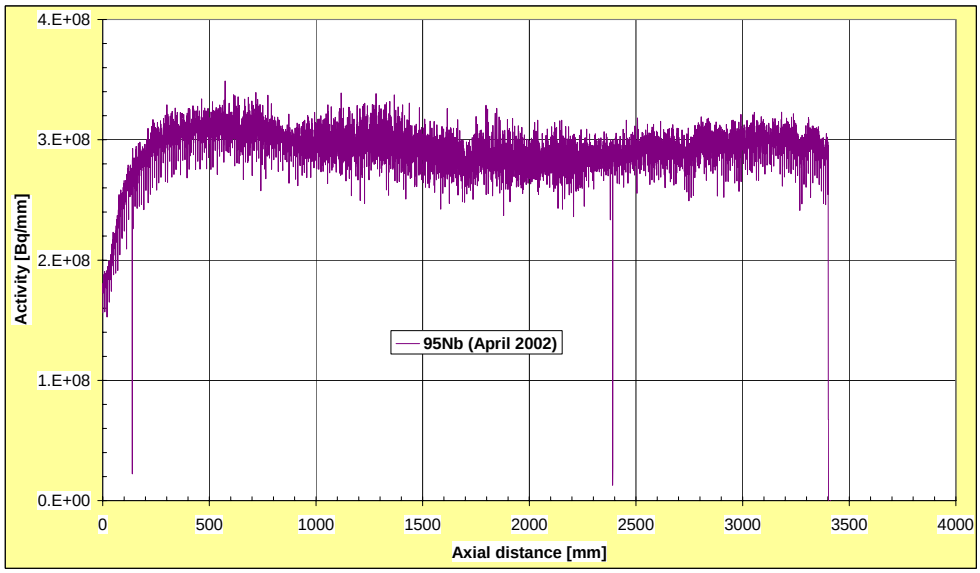

Figure 6 Rod WZR0058, axial ^{95}Nb activity distribution at the time of measurement (April 2002)

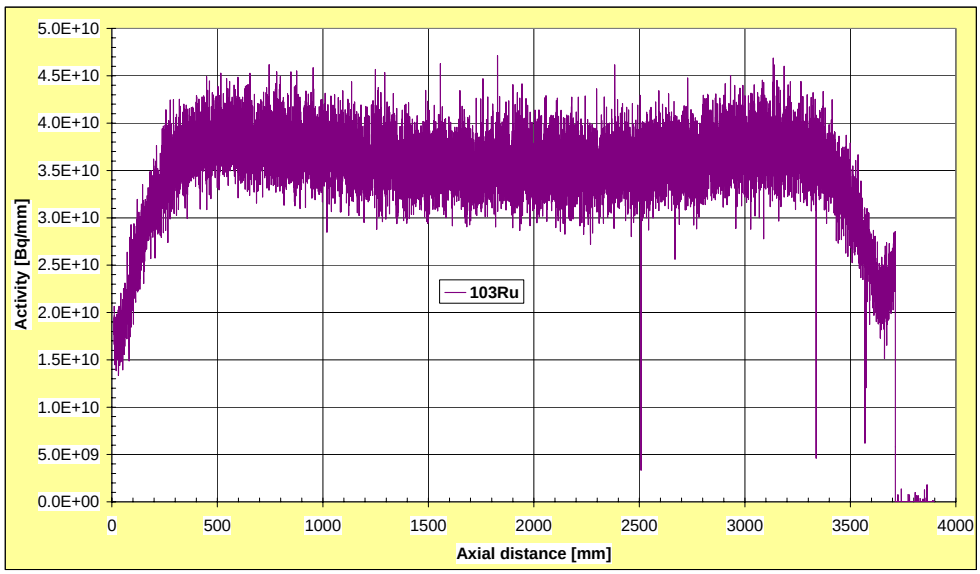

Figure 7 Rod WZtR165, axial ^{103}Ru activity distribution at the end of irradiation

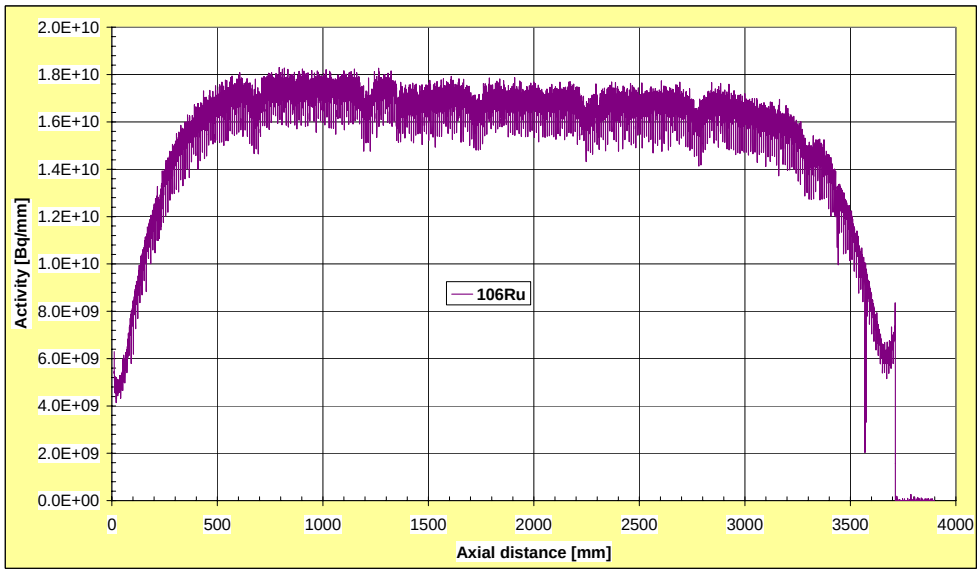

Figure 8 Rod WZtR165, axial ^{106}Ru activity distribution at the end of irradiation

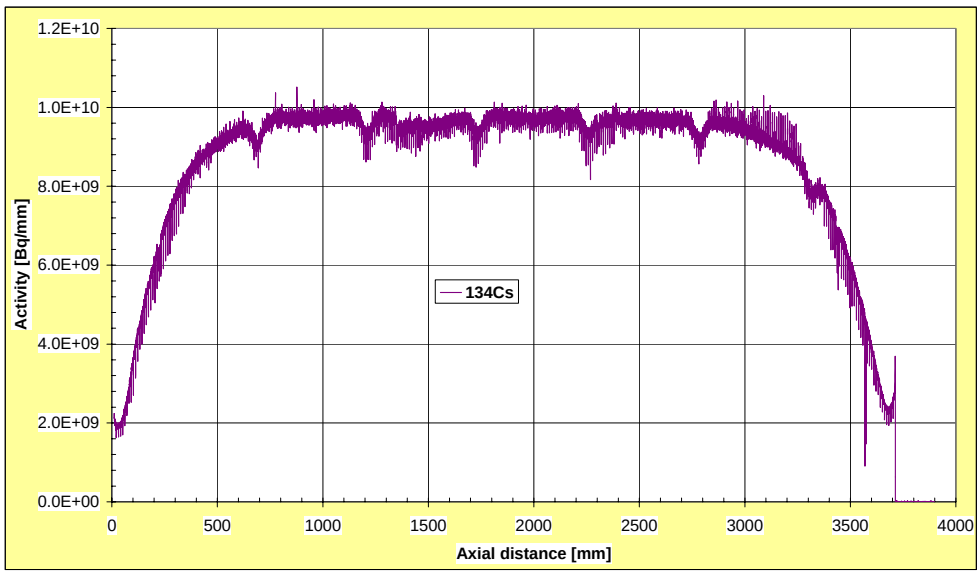

Figure 9 Rod WZtR165, axial ^{134}Cs activity distribution at the end of irradiation

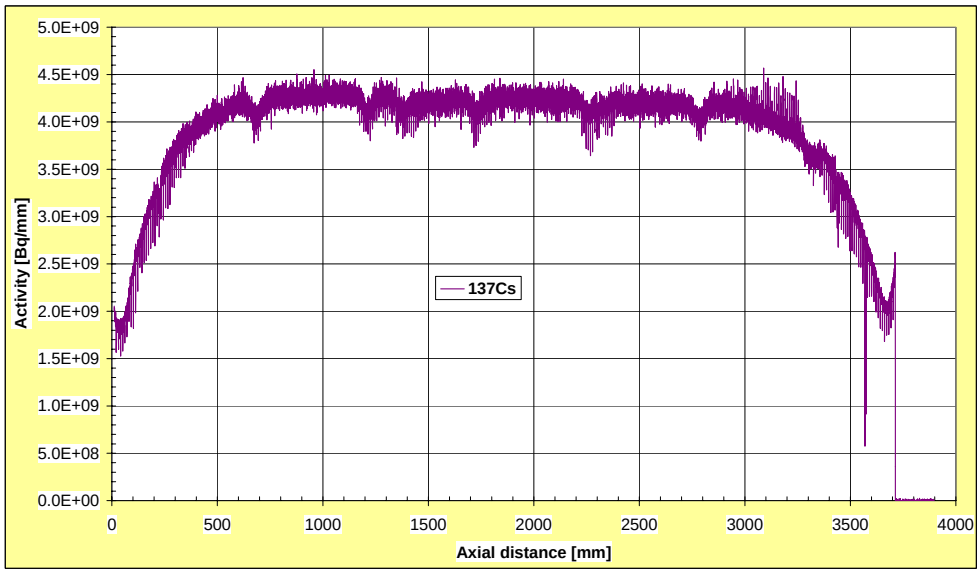

Figure 10 Rod WZtR165, axial ^{137}Cs activity distribution at the end of irradiation

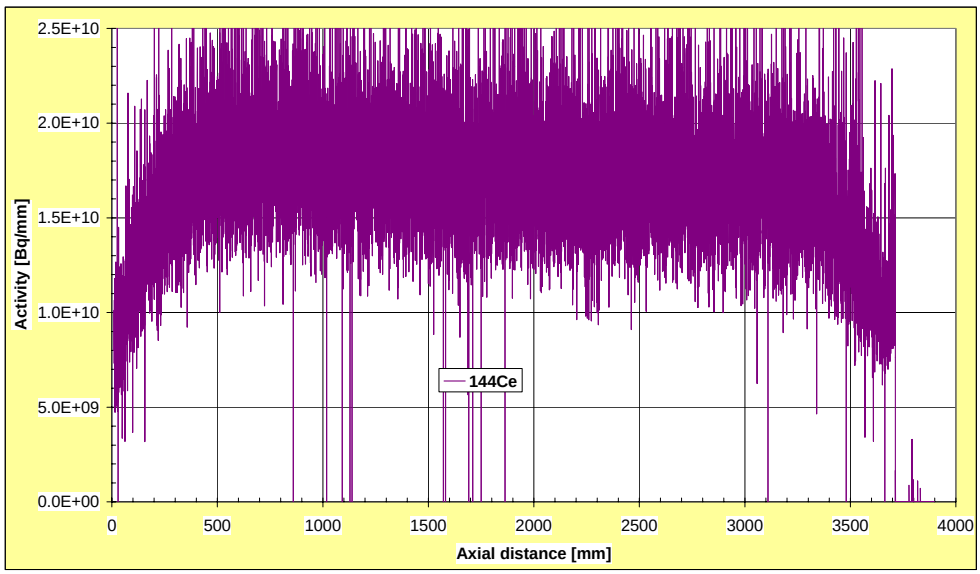

Figure 11 Rod WZtR165, axial ^{144}Ce activity distribution at the end of irradiation

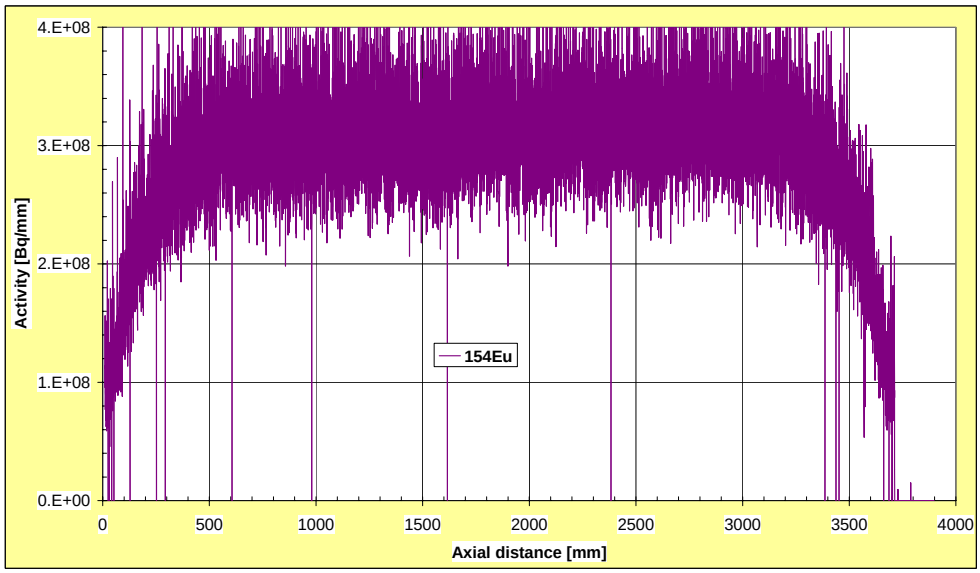

Figure 12 Rod WZtR165, axial ^{154}Eu activity distribution at the end of irradiation

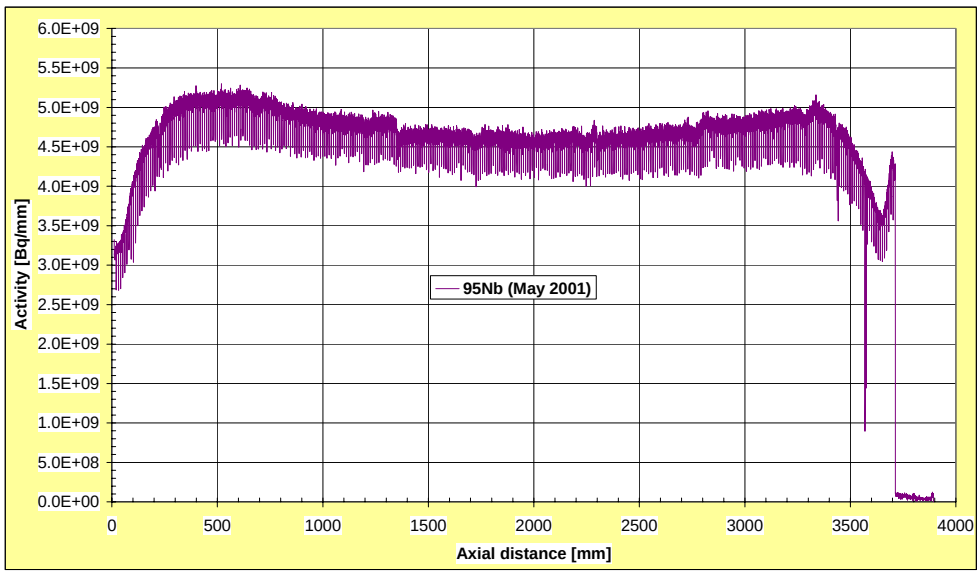

Figure 13 Rod WZtR165, axial ^{95}Nb activity distribution at the time of measurement (May 2001)

Table 5 Estimated nuclide and rod specific single point standard deviations

Isotope	WZtR165	WZR0058
^{144}Ce	13,6 %	5,47 %
^{103}Ru	7,53 %	
^{106}Ru	1,63 %	1,91 %
^{134}Cs	0,85 %	1,03 %
^{137}Cs	1,48 %	1,11 %
^{154}Eu	10,75 %	4,72 %
^{144}Pr	13,91 %	11,97 %
^{137m}Ba	1,48 %	1,11 %
^{95}Nb	1,31 %	3,36 %

Table 6 Estimated nuclide and rod specific overall errors

Isotope	WZtR165	WZR0058
^{144}Ce	19,0 %	14,0 %
^{103}Ru	15,2 %	
^{106}Ru	13,3 %	13,0 %
^{134}Cs	13,3 %	12,9 %
^{137}Cs	13,3 %	12,9 %
^{154}Eu	17,1 %	13,7 %
^{144}Pr	19,2 %	17,6 %
^{137m}Ba	13,3 %	12,9 %
^{95}Nb	13,3 %	13,3 %

3.3 $^{n}X/^{238}U$ Values based on Gamma Scanning

$^{n}X/^{238}U$ values based on gamma scanning are compiled in Table 7. The indicated error is calculated from the standard deviation of the mean value of the activity calculated according to paragraph 2.3.3 and the estimated single errors indicated in Table 6, applying the rules of error propagation. Selected values are plotted in Figure 17 and Figure 18 as a function of the burnup shown in Table 1. The fact that all values for samples E58-773, E58-793 and E58-796 are almost identical and very close to the corresponding values of sample WZtR165-2a indicates that at least some of the single errors shown in Table 6 are probably greatly overestimated.

3.4 $^{n}X/^{238}U$ Values based on One-Point Calibration

$^{n}X/^{238}U$ values determined by ICP-MS analysis based one-point calibration are compiled in Table 8. The indicated errors are estimated based on experience when analysing samples with known composition with this method. ^{135}Cs is determined on the basis of ^{133}Cs and the ratio of the respective count rates. Selected values are plotted in Figure 17 and Figure 18 as well as a function of the burnup shown in Table 1.

When judging the ^{133}Cs results, it should be kept in mind that the mother nuclide ^{133}Xe has a half-life of 5.25 days. This half-life may be long enough to release some ^{133}Xe into the free volume of the rod before it has decayed into ^{133}Cs. This effect would be fuel temperature dependent and thus somewhat more pronounced in high burnup samples.

In the case of ^{135}Cs, the mother nuclide ^{135}Xe has a very large thermal neutron cross section (2.65×10^{6} barn). The amount of ^{135}Xe that is not transformed into ^{136}Xe, but decays to ^{135}Cs is therefore strongly dependent on the neutron spectrum.

^{244}Cm has a half-life of 18.1 years. A significant amount present at the end of bombardment (EOB) has already decayed. Therefore, the analysed values are presented together with values calculated back to September 2000.

3.5 $^{n}X/^{238}U$ Values based on Isotope Dilution Analysis

$^{n}X/^{238}U$ values determined by ICP-MS and HPLC-ICP-MS by means of IDA are compiled in Table 9. The indicated errors are calculated as described on page 8. Selected data are plotted against the burnup shown in Table 1 in Figure 14 to Figure 23.

In general, the sets of data are consistent. When comparing data from samples with a burnup around 75 MWd/kgU with results from samples with lower burnup, it should be kept in mind that irradiating conditions, in particular the neutron spectrum, may have been different towards the end of the rod, where the low burnup samples stem from.

^{144}Ce/Pr (half-life 284.8 d) decays into ^{144}Nd. Based on the amount of ^{144}Ce present at EOB determined by gamma spectrometry, it is possible to calculate the amount of ^{144}Nd present at EOB.

In addition to the errors indicated in Table 9, systematic errors can not be excluded. Potential sources for systematic errors are for instance:

- Erroneous concentration of spike atom concentration. A sample taken adjacent to an irradiated fuel sample that had been analysed independently by different laboratories was analysed in the same campaign as the Vandellos samples. The first results indicated that the concentration of the ^{140}Ce spike solution was probably about 10 % higher than analysed by an independent analytical laboratory. On the other hand, there were indications that the neodymium spike concentration might have been about 10 % lower than analysed by the same laboratory. This was confirmed after editing of Rev. 0 of the present report. Control analyses of spike solution also revealed an erroneous Eu spike concentration. Corrected results can be found in Table 4 of [Ref. 3].
- Mass bias of the ICP-MS instrument, although the analysis of a mixture of lanthanides with natural isotopic composition did not reveal any bias larger than the variations taken into account in the error calculation.
- Erroneous dead time correction in the uranium analysis. The result from the sample analysed together with the ENUSA samples that had been analysed independently by other methods indicates that the applied dead time is correct.
- The evaluation program MassLynx, applied for determining the peak areas in HPLC-ICP-MS analyses. Fitting parameters in MassLynx data evaluations are manually adjusted. A certain influence of the human factor on the result of the evaluations can therefore not be excluded, in particular when assessing small peak areas. $^{n}X/^{238}$U weight ratios smaller than about 0.05 % may therefore be systematically high or low by up to about 10 % (relative), compared to larger values of the same element. The direction of the deviation is not obvious, as it depends on the choice of individual evaluating parameters.

3.6 Burnup Determination

Regarding burnup determination, it is referred to Section 3.2 of [Ref. 3].

Table 7 $^{n}X/^{238}U$ **values based on gamma scanning**

Sample	E58-88	E58-148	E58-263	E58-773	E58-793	E58-796	WZtR165-2a
Residual ^{238}U [%]	97.0	96.1	95.1	94.0	94.0	94.0	93.9
$^{103}Ru/^{238}U$ [%]	Below detection limit after long cooling time						0.0071 ± 0.0011
$^{106}Ru/^{238}U$ [%]	0.015 ± 0.002	0.020 ± 0.003	0.026 ± 0.003	0.032 ± 0.004	0.032 ± 0.004	0.032 ± 0.004	0.033 ± 0.004
$^{134}Cs/^{238}U$ [%]	0.017 ± 0.002	0.024 ± 0.003	0.034 ± 0.005	0.045 ± 0.006	0.045 ± 0.006	0.045 ± 0.006	0.047 ± 0.006
$^{137}Cs/^{238}U$ [%]	0.171 ± 0.011	0.211 ± 0.012	0.254 ± 0.014	0.300 ± 0.017	0.300 ± 0.017	0.300 ± 0.017	0.307 ± 0.020
$^{144}Ce/^{238}U$ [%]	0.0205 ± 0.0029	0.0245 ± 0.0034	0.0288 ± 0.0040	0.0325 ± 0.0045	0.0328 ± 0.0045	0.0328 ± 0.0045	0.0344 ± 0.0071
$^{154}Eu/^{238}U$ [%]	0.00343 ± 0.00049	0.00451 ± 0.00064	0.00556 ± 0.00075	0.00650 ± 0.00089	0.00649 ± 0.00089	0.00649 ± 0.00089	0.00724 ± 0.00135
$^{95}Nb/^{238}U$ [%](1)	(3.8±0.6)E-5	(4.2±0.6)E-5	(4.7±0.7)E-5	(4.8±0.7)E-5	(4.8±0.7)E-5	(4.8±0.7)E-5	0.00076 ± 0.00011

(1) At time of measurement

Table 8 $^{n}X/^{238}U$ **values determined by ICP-MS analysis based on one-point calibration (date of analysis: October 24, 2003)**

Sample	E58-88	E58-148	E58-263	E58-773	E58-793	E58-796	WZtR165-2a
$^{133}Cs/^{238}U$ [%]	0.162±0.013	0.183±0.014	0.228±0.018	0.237±0.019	0.219±0.017	0.221±0.017	0.219±0.017
$^{135}Cs/^{238}U$ [%]	0.089±0.007	0.103±0.008	0.118±0.010	0.111±0.009	0.101±0.008	0.103±0.008	0.114±0.010
$^{237}Np/^{238}U$ [%]	0.073±0.006	0.100±0.008	0.130±0.011	0.127±0.010	0.117±0.009	0.122±0.010	0.140±0.011
$^{244}Cm/^{238}U$ [%] (at EOB)	0.0019±0.0002 0.0022	0.0060±0.0006 0.0067	0.0151±0.0015 0.0170	0.0234±0.0023 0.0264	0.0221±0.0022 0.0249	0.0227±0.0023 0.0255	0.0291±0.0029 0.0327
$^{246}Cm/^{238}U$ [%]	0.000018±0.000004	0.000062±0.000012	0.00025±0.00004	0.00057±0.00009	0.00053±0.00009	0.00054±0.00009	0.00073±0.00012

Table 9 $^{n}X/^{238}U$ values based isotope dilution analysis (analyses performed in October 2003)

Sample	E58-88	E58-148	E58-263	E58-773	E58-793	E58-796	WZtR165-2a
$^{233}U/^{238}U$ [%]	<0.005	<0.005	<0.005	<0.005	<0.005	<0.005	<0.005
$^{234}U/^{238}U$ [%]	0.0245 ± 0.0022	0.0232 ± 0.0017	0.0161 ± 0.0032	0.0136 ± 0.0018	0.0150 ± 0.0033	0.0152 ± 0.0019	0.0140 ± 0.0019
$^{235}U/^{238}U$ [%]	1.328 ± 0.074	0.921 ± 0.032	0.525 ± 0.036	0.321 ± 0.016	0.312 ± 0.027	0.320 ± 0.015	0.294 ± 0.013
$^{236}U/^{238}U$ [%]	0.568 ± 0.028	0.687 ± 0.025	0.677 ± 0.045	0.645 ± 0.029	0.684 ± 0.047	0.671 ± 0.025	0.681 ± 0.025
$^{238}Pu/^{238}U$ [%]	0.0281 ± 0.0010	0.0402 ± 0.0027	0.0651 ± 0.0035	0.0884 ± 0.0042	0.0977 ± 0.0068	0.0859 ± 0.0050	0.0971 ± 0.0048
$^{239}Pu/^{238}U$ [%]	0.652 ± 0.016	0.642 ± 0.022	0.640 ± 0.032	0.676 ± 0.023	0.724 ± 0.042	0.679 ± 0.024	0.741 ± 0.022
$^{240}Pu/^{238}U$ [%]	0.250 ± 0.006	0.293 ± 0.010	0.327 ± 0.016	0.372 ± 0.013	0.395 ± 0.026	0.385 ± 0.014	0.404 ± 0.013
$^{241}Pu/^{238}U$ [%]	0.140 ± 0.004	0.160 ± 0.006	0.182 ± 0.009	0.199 ± 0.007	0.216 ± 0.015	0.205 ± 0.009	0.221 ± 0.007
$^{242}Pu/^{238}U$ [%]	0.0574 ± 0.0016	0.0920 ± 0.0033	0.1370 ± 0.0069	0.1864 ± 0.0068	0.1994 ± 0.0138	0.1853 ± 0.0072	0.2095 ± 0.0065
$^{241}Am/^{238}U$ [%]	0.0260 ± 0.0010	0.0288 ± 0.0009	0.0321 ± 0.0017	0.0360 ± 0.0014	0.0306 ± 0.0015	0.0326 ± 0.0009	0.0371 ± 0.0010
$^{243}Am/^{238}U$ [%]	0.0093 ± 0.0004	0.0245 ± 0.0015	0.0418 ± 0.0035	0.0634 ± 0.0026	0.0510 ± 0.0029	0.0649 ± 0.0027	0.0766 ± 0.0020
$^{140}Ce/^{238}U$ [%]	See Table 4 of [Ref. 3]						
$^{142}Ce/^{238}U$ [%]							
$^{142}Nd/^{238}U$ [%]	See Table 4 of [Ref. 3]						
$^{143}Nd/^{238}U$ [%]							
$^{144}Nd/^{238}U$ [%] (at EOB)							
$^{145}Nd/^{238}U$ [%]							
$^{146}Nd/^{238}U$ [%]							
$^{148}Nd/^{238}U$ [%]							
$^{150}Nd/^{238}U$ [%]							

Table 9 $^{nX/238U}$ values based isotope dilution analysis (continued)

Sample	E58-88	E58-148	E58-263	E58-773	E58-793	E58-796	WZtR165-2a
$^{147}Sm/^{238}U$ [%]	0.0284 ± 0.0008	0.0297 ± 0.0007	0.0282 ± 0.0013	0.0282 ± 0.0013	0.0298 ± 0.0014	0.0286 ± 0.0008	0.0319 ± 0.0010
$^{148}Sm/^{238}U$ [%]	0.0204 ± 0.0005	0.0300 ± 0.0007	0.0373 ± 0.0017	0.0506 ± 0.0023	0.0543 ± 0.0025	0.0498 ± 0.0012	0.0565 ± 0.0017
$^{149}Sm/^{238}U$ [%]	0.00036 ± 0.00003	0.00039 ± 0.00003	0.00032 ± 0.00002	0.00038 ± 0.00003	0.00040 ± 0.00003	0.00042 ± 0.00004	0.00039 ± 0.00005
$^{150}Sm/^{238}U$ [%]	0.0353 ± 0.0010	0.0472 ± 0.0011	0.0529 ± 0.0024	0.0675 ± 0.0030	0.0709 ± 0.0032	0.0649 ± 0.0016	0.0659 ± 0.0020
$^{151}Sm/^{238}U$ [%]	0.00149 ± 0.00008	0.00154 ± 0.00006	0.00154 ± 0.00007	0.00192 ± 0.00010	0.00203 ± 0.00011	0.00194 ± 0.00005	0.00192 ± 0.00010
$^{152}Sm/^{238}U$ [%]	0.0132 ± 0.0003	0.0155 ± 0.0003	0.0164 ± 0.0007	0.0193 ± 0.0008	0.0199 ± 0.0009	0.0195 ± 0.0005	0.0204 ± 0.0005
$^{154}Sm/^{238}U$ [%]	0.00426 ± 0.00016	0.00563 ± 0.00015	0.00678 ± 0.00031	0.00872 ± 0.00041	0.00911 ± 0.00042	0.00917 ± 0.00028	0.01185 ± 0.00050
$^{151}Eu/^{238}U$ [%]	See Table 4 of [Ref. 3]						
$^{153}Eu/^{238}U$ [%]							
$^{154}Eu/^{238}U$ [%] (at EOB)							
$^{155}Eu/^{238}U$ [%]							
$^{154}Gd/^{238}U$ [%]	0.00101 ± 0.00005	0.00154 ± 0.00007	0.00170 ± 0.00010	0.00236 ± 0.00008	0.00236 ± 0.00014	0.00224 ± 0.00007	0.00281 ± 0.00024
$^{155}Gd/^{238}U$ [%]	3.0E-04 ± 2.5E-05	4.9E-04 ± 4.0E-05	5.5E-04 ± 2.6E-05	7.8E-04 ± 3.4E-05	7.5E-04 ± 4.0E-05	6.8E-04 ± 2.0E-05	6.1E-04 ± 2.8E-05
$^{156}Gd/^{238}U$ [%]	0.00988 ± 0.00028	0.01918 ± 0.00088	0.02925 ± 0.00134	0.04849 ± 0.00165	0.04963 ± 0.00222	0.04720 ± 0.00115	0.04963 ± 0.00228
$^{157}Gd/^{238}U$ [%]	<1E-06	<1E-06	<1E-06	<1E-06	<1E-06	<1E-06	<1E-06
$^{158}Gd/^{238}U$ [%]	0.00170 ± 0.00007	0.00301 ± 0.00016	0.00423 ± 0.00019	0.00720 ± 0.00025	0.00723 ± 0.00035	0.00684 ± 0.00018	0.00738 ± 0.00045
$^{160}Gd/^{238}U$ [%]	0.00014 ± 0.00001	0.00018 ± 0.00003	0.00024 ± 0.00001	0.00039 ± 0.00006	0.00031 ± 0.00006	0.00028 ± 0.00001	0.00039 ± 0.00002

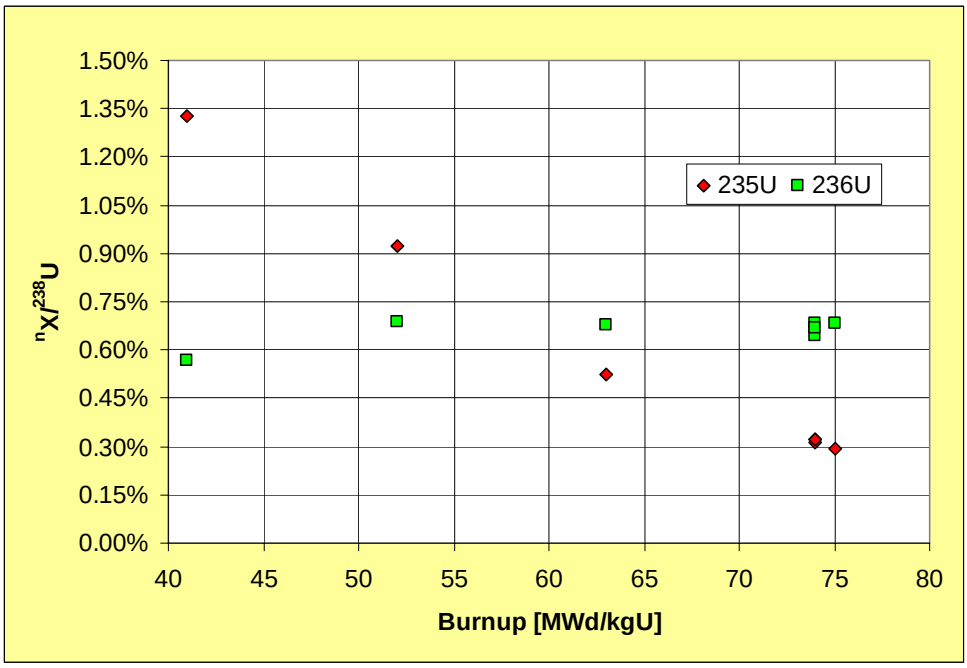

Figure 14 **$^{n}U/^{238}U$ values as a function of burnup based on gamma scan**

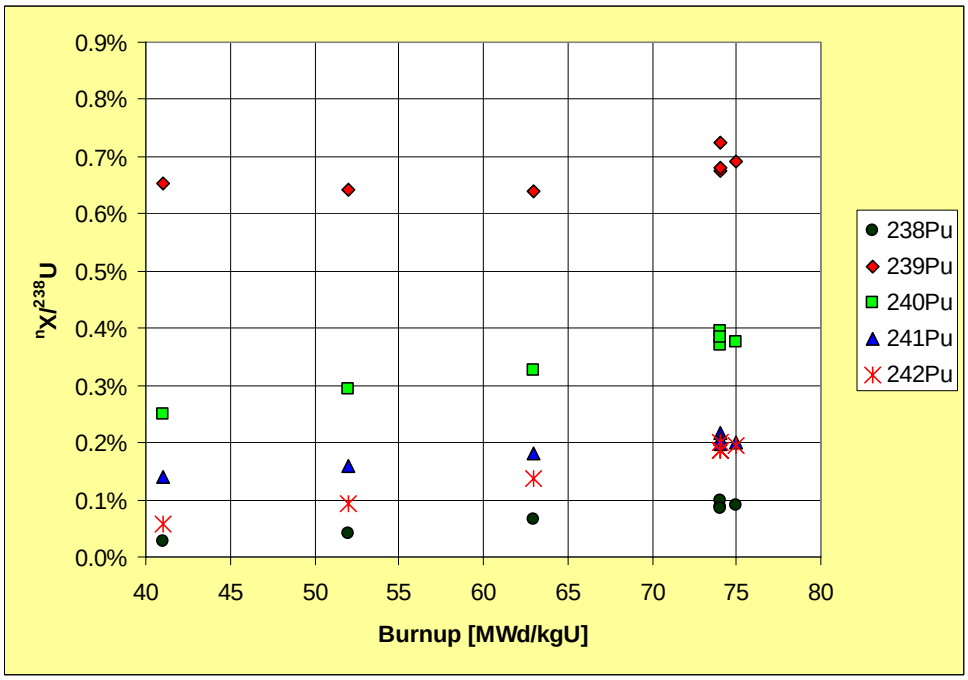

Figure 15 **$^{n}Pu/^{238}U$ values as a function of burnup based on gamma scan**

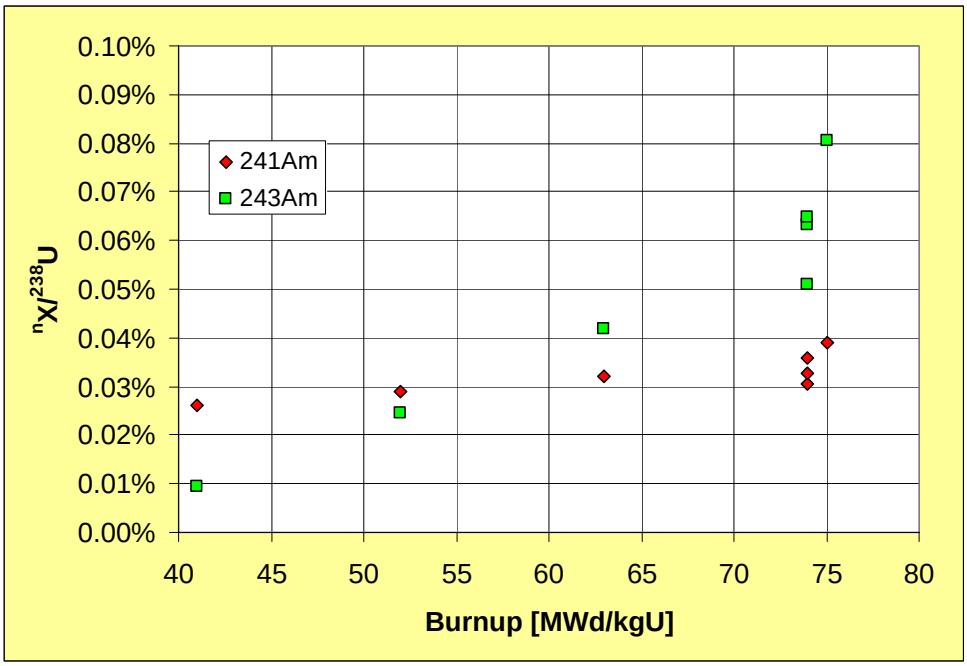

Figure 16 **^{n}Am/^{238}U values as a function of burnup based on gamma scan**

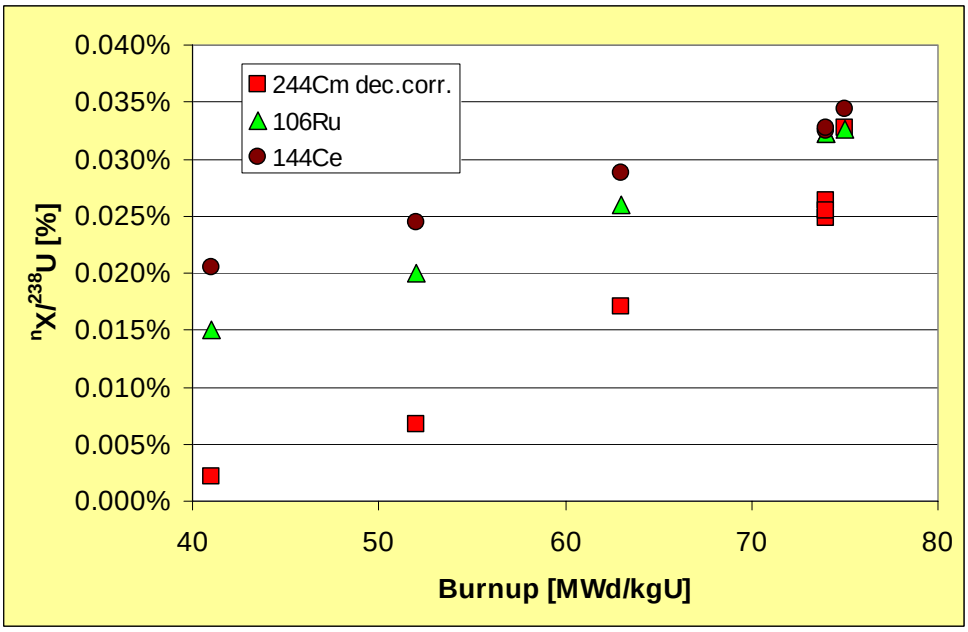

Figure 17 **^{106}Ru/^{238}U, ^{144}Ce/^{238}U and ^{244}Cm/^{238}U values as a function of burnup based on gamma scan**

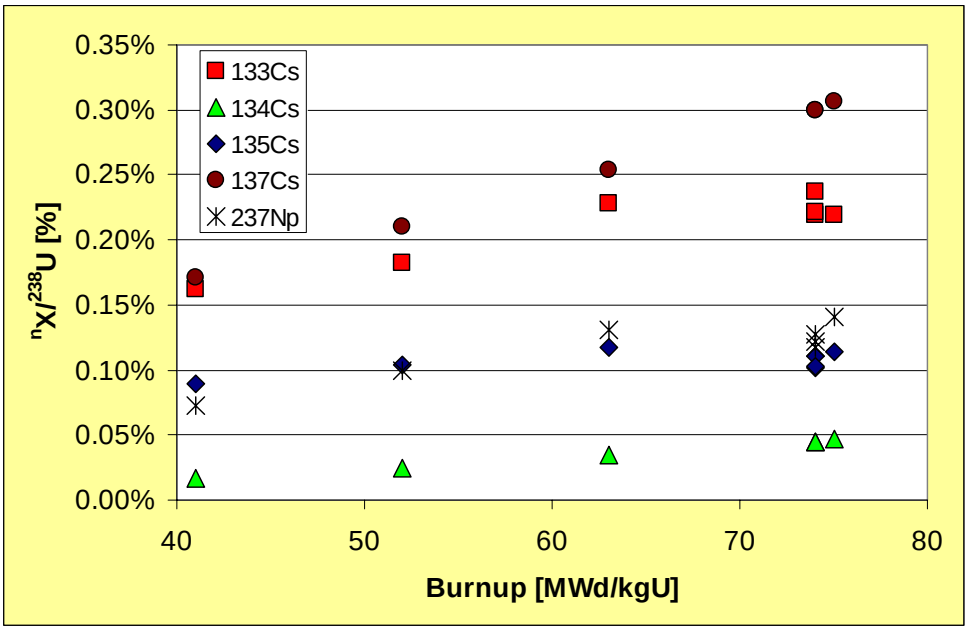

Figure 18 **^{n}Cs/^{238}U and ^{237}Np/^{238}U values as a function of burnup based on gamma scan**

See Figure 6 of [Ref. 3]

Figure 19 **$^{140, 142}$Ce/^{238}U values as a function of burnup based on gamma scan**

See Figure 7 of [Ref. 3]

Figure 20 **^{n}Nd/^{238}U values as a function of burnup based on gamma scan**

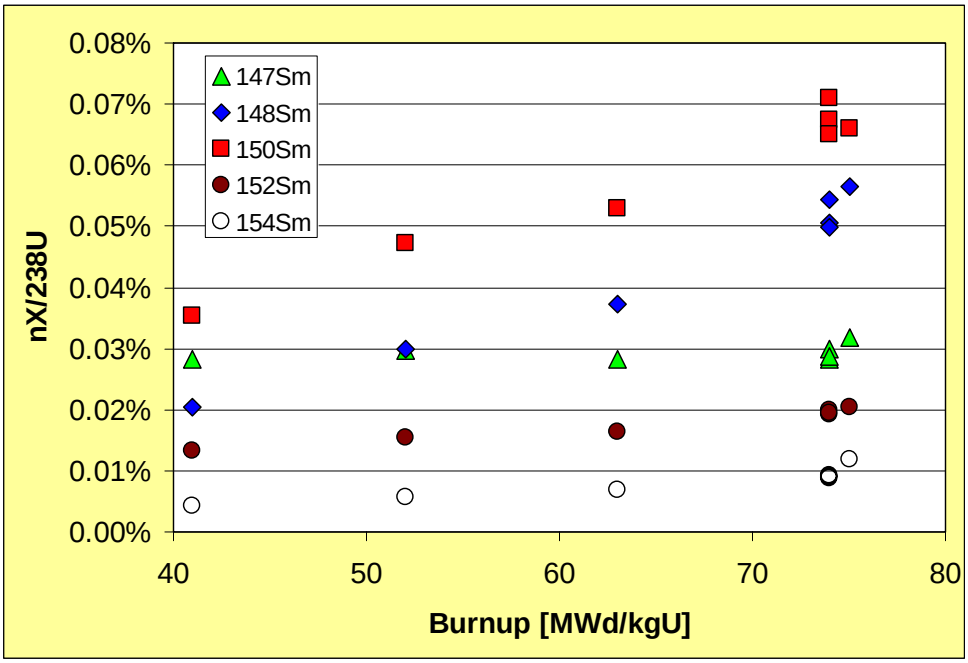

Figure 21 **^{n}Sm/^{238}U values as a function of burnup based on gamma scan**

See Figure 9 of [Ref. 3]

Figure 22 $^{n}Eu/^{238}U$ values as a function of burnup based on gamma scan

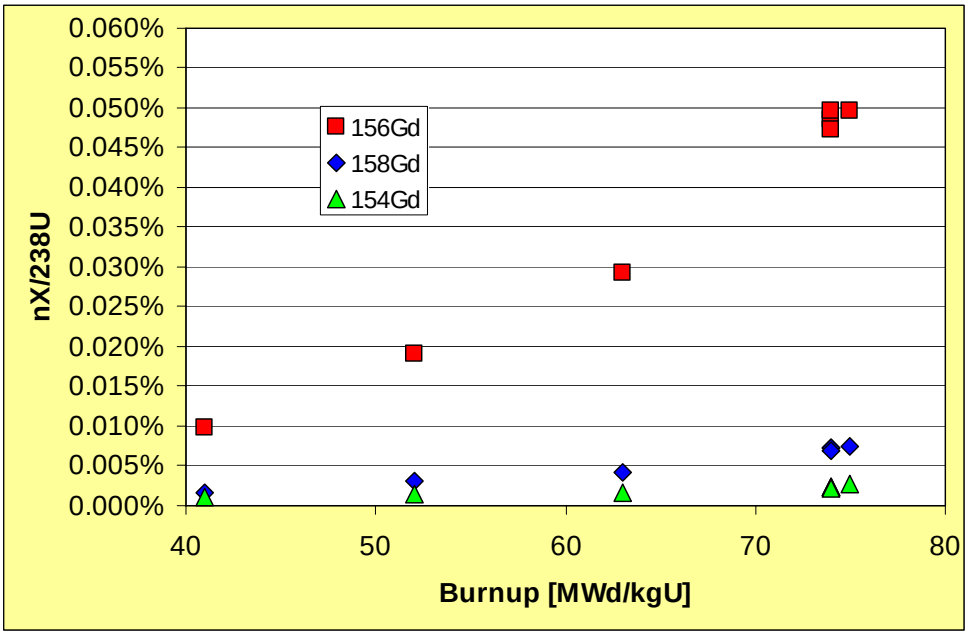

Figure 23 $^{n}Gd/^{238}U$ values as a function of burnup based on gamma scan

4 Conclusions

Over 40 nuclides have been analysed by ICP-MS in 7 different irradiated fuel samples. In addition, about 10 nuclides were determined based on axial gamma scans of the two rods WZR0058 and WZtR165. In general, these over 300 data points give a consistent picture of the isotopic content of irradiated fuel as a function of burnup. Taking into account that Studsvik applied these methods for the first time in such a comprehensive project, the outcome is considered to be satisfactory. On the other hand, some systematic deviations from expectations have been identified. Moreover, the scatter of $^{n}X/^{238}$U weight ratios of fission products that would have the potential for determining the local pellet burnup by comparison with CASMO calculations appears to be too large. Therefore, burnup values determined by comparing the isotopic abundance of ^{235}U and ^{239}Pu to CASMO based values are considered to be the most reliable ones.

Some apparent systematic errors could be eliminated by additional analyses performed after editing of Rev. 0 of this report. Revised results can be found in [Ref. 3].

5 Acknowledgements

Cutting and dissolution of the samples has been performed by the staff of the Studsvik hotcell laboratory, in particular Max Lundström, Vanja Liljedal and Leif Kjellberg.

Jesper Kierkegaard and Erik-Bertil Jonsson carried out the CASMO calculations that formed the basis for burnup determinations.

Additional employees of Studsvik Nuclear, contributing with discussions, ideas and valuable reviewing comments to the successful completion of the project include Gunnar Lysell, David Schrire, Francesco Corleoni, Björn Andersson and Hans Johansson.

Last but not least, the support by ENUSA, in particular through Pekka Tolonen and Manuel Quecedo, and their understanding for experimental difficulties leading to severe delays is very much appreciated.

References

Ref. 1 Monika Källberg, Anders Thanger, Hans-Urs Zwicky, *Characterisation of plenum samples cut from high burnup rods irradiated in Vandellos 2*, Studsvik Report N-08/041, 2008-02-15

Ref. 2 Anna Dormann, *The arrival and unloading of the fuel rods from Vandellos at Studsvik in March 2001*, Studsvik Technical Note N-07/191, 2008-01-29

Ref. 3 Hans-Urs Zwicky, Jeanett Low, *Fuel Pellet Isotopic Analyses of Vandellós 2 Rods WZtR165 and WZR0058*: Complementary Report, Studsvik Technical Note N-04/135 Rev. 1, 2008-04-25

Ref. 4 QUECEDO, M
Personal communication to Erik Bertil Jonsson
COM-006998, Rev. 0,
September 6, 2002

Ref. 5 LERAY, U, CORLEONI, F
Vandellos Irradiation Extension Program: Visual check before cutting, rod length, puncture/FGR and final cutting positions,
Studsvik Nuclear AB Technical Note N(H)-01/062, Rev. 1
2008-02-28

Ref. 6 CORLEONI, F
Pellet isotopic analysis of Vandellos II rods WZtR165 and WZR0058 by gamma measurements,
Studsvik Nuclear AB Technical Note N(H)-03/026, Rev. 1
2008-03-06

Ref. 7 RÖLLIN, S, et al.
Determination of lanthanides in uranium materials using high performance liquid chromatographic separation and ICP-MS detection,
"Recent Advances in Plasma Source Mass Spectrometry" (Ed. G. Holland), 28-35, 1994

Ref. 8 JARVIS, K E, GRAY, A L,
Handbook of ICP-MS
ISBN 0-216-92912-1

Ref. 9 *Standard test method for atom percent fission in uranium and plutonium fuel (Neodymium-148 method*)
ASTM Standard E-321-96

Ref. 10 *Standard test method for atom percent fission in uranium and plutonium fuel (mass pectrometric method)*
ASTM Standard E 244-80(1995) (Withdrawn 2001)

Revision Record

Rev. No.	Revised by	Reviewed by	Approved by	Date
0		Gunnar Lysell	Hans Johansson	2004-03-08
1	Hans-Urs Zwicky	Gunnar Lysell	Camilla Hoflund	2008-04-25

Rev. No.	Section	Description of revision
1	Summary, Introduction	Reason for Revision explained
1	All	Rod and sample designations replaced
1	Results and Discussion	Erroneous text, data and figures deleted and replaced by reference to complementary report [Ref. 3]